

# UC San Diego

## UC San Diego Previously Published Works

### Title

A substitution in cGMP-dependent protein kinase 1 associated with aortic disease induces an active conformation in the absence of cGMP

### Permalink

<https://escholarship.org/uc/item/4953d61k>

### Journal

Journal of Biological Chemistry, 295(30)

### ISSN

0021-9258

### Authors

Chan, Matthew H  
Aminzai, Sahar  
Hu, Tingfei  
et al.

### Publication Date

2020-07-01

### DOI



10.1074/jbc.ra119.010984

Peer reviewed



# A substitution in cGMP-dependent protein kinase 1 associated with aortic disease induces an active conformation in the absence of cGMP

Received for publication, September 6, 2019, and in revised form, June 4, 2020. Published, Papers in Press, June 5, 2020, DOI 10.1074/jbc.RA119.010984

Matthew H. Chan<sup>1</sup>, Sahar Aminzai<sup>1</sup>, Tingfei Hu<sup>1</sup>, Amatya Taran<sup>1</sup>, Sheng Li<sup>1</sup>, Choel Kim<sup>2</sup> , Renate B. Pilz<sup>1</sup> , and Darren E. Casteel<sup>1,\*</sup>

From the <sup>1</sup>Department of Medicine, University of California, San Diego, La Jolla, California, USA and <sup>2</sup>Verna and Marris McLean Department of Biochemistry and Molecular Biology and the Department of Pharmacology and Chemical Biology, Baylor College of Medicine, Houston, Texas, USA

Edited by Roger J. Colbran

Type 1 cGMP-dependent protein kinases (PKGs) play important roles in human cardiovascular physiology, regulating vascular tone and smooth-muscle cell phenotype. A mutation in the human PRKG1 gene encoding cGMP-dependent protein kinase 1 (PKG1) leads to thoracic aortic aneurysms and dissections. The mutation causes an arginine-to-glutamine (RQ) substitution within the first cGMP-binding pocket in PKG1. This substitution disrupts cGMP binding to the pocket, but it also unexpectedly causes PKG1 to have high activity in the absence of cGMP via an unknown mechanism. Here, we identified the molecular mechanism whereby the RQ mutation increases basal kinase activity in the human PKG1 $\alpha$  and PKG1 $\beta$  isoforms. Although we found that the RQ substitution (R177Q in PKG1 $\alpha$  and R192Q in PKG1 $\beta$ ) increases PKG1 $\alpha$  and PKG1 $\beta$  autophosphorylation *in vitro*, we did not detect increased autophosphorylation of the PKG1 $\alpha$  or PKG1 $\beta$  RQ variant isolated from transiently transfected 293T cells, indicating that increased basal activity of the RQ variants in cells was not driven by PKG1 autophosphorylation. Replacement of Arg-177 in PKG1 $\alpha$  with alanine or methionine also increased basal activity. PKG1 exists as a parallel homodimer linked by an N-terminal leucine zipper, and we show that the WT chain in WT-RQ heterodimers partly reduces basal activity of the RQ chain. Using hydrogen/deuterium-exchange MS, we found that the RQ substitution causes PKG1 $\beta$  to adopt an active conformation in the absence of cGMP, similar to that of cGMP-bound WT enzyme. We conclude that the RQ substitution in PKG1 increases its basal activity by disrupting the formation of an inactive conformation.

The type 1 cGMP-dependent protein kinases play key roles in the cardiovascular system, including modulation of vascular tone, inhibition of thrombosis, and protection from cardiac hypertrophy/fibrosis. (1). At the cellular level, protein kinase G (PKG) regulates intracellular calcium concentrations and the contractile machinery's sensitivity to calcium; PKG also controls gene transcription and apoptosis (2). The kinases are downstream effectors of the natriuretic peptide/nitric oxide (NO)-guanylate cyclase signaling pathways and are the targets of drugs that raise intracellular cGMP levels by releasing NO,

directly activating guanylate cyclase, or inhibiting cGMP breakdown (3).

Mammalian cells express two PKG1 isoforms, PKG1 $\alpha$  and PKG1 $\beta$ , which are produced from alternative transcriptional start utilization and/or alternate splicing from the same gene; they differ in their first ~100 amino acids (1). PKG1 is a single-chain kinase with an N-terminal regulatory domain and a C-terminal catalytic domain (Fig. 1A). The regulatory domain can be further divided into functional subdomains. Located at the very N terminus are isoform-specific leucine/isoleucine zipper (LZ) domains, which mediate homodimerization and target the PKG1 isoforms to specific substrates (4–10). The LZ domains are followed by isoform-specific autoinhibitory (AI) domains, which contain pseudosubstrate sequences and inhibit kinase activity by binding within the catalytic cleft to block substrate access. The AI domains also contain autophosphorylation sites that can activate the kinases in the absence of cGMP, *i.e.* autophosphorylation of S<sup>65</sup> in PKG1 $\alpha$  and S<sup>80</sup> in PKG1 $\beta$  leads to cGMP-independent kinase activation (11, 12). Whereas the N termini are unique, PKG1 $\alpha$  and PKG1 $\beta$  have identical cyclic nucleotide binding (CNB-A and CNB-B) and catalytic domains. PKG is activated by a cGMP-induced conformational change in the regulatory domain, which pulls the pseudosubstrate sequence from the catalytic cleft (13). The cGMP-induced exposure of the catalytic cleft in PKG1 $\alpha$  has been previously shown using hydrogen/deuterium exchange MS (H/DX-MS) (13).

In humans, a mutation in the gene for PKG1 causes familial thoracic aortic aneurysms and dissections (14). The mutation changes a conserved arginine residue in CNB-A to glutamine and causes a high basal kinase activity in the absence of cGMP (R177Q in PKG1 $\alpha$  and R192Q in PKG1 $\beta$ ) (14). A knock-in mouse heterozygous for the same mutation develops age-dependent aortic dilatation and aortic media degeneration with elastin fiber breaks (15). Whereas the mutation causes an ~32,000-fold lower cGMP affinity in CNB-A, the mutant kinase has the same  $V_{\max}$  as the WT enzyme under saturating cGMP conditions (14). Exactly how the RQ mutation leads to PKG1 activation is unknown. In the current study, we describe some unique biochemical properties of the mutant kinase, and we used H/DX-MS to compare the conformations of WT and R192Q PKG1 $\beta$  in the absence and presence of cGMP. We

This article contains supporting information.

\* For correspondence: Darren E. Casteel, [dcasteel@ucsd.edu](mailto:dcasteel@ucsd.edu).

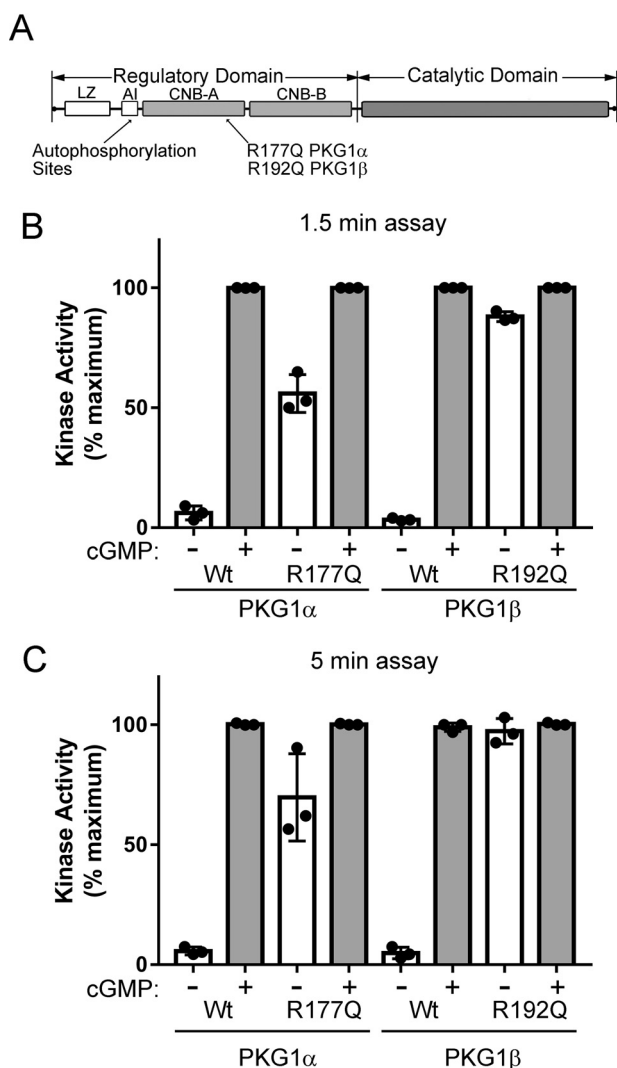


**Figure 1.** *In vitro* kinase activity of PKG1 $\alpha$  R177Q and PKG1 $\beta$  R192Q. **A**, domain organization of PKG1 highlighting the locations of autophosphorylation sites and the activating RQ mutation. The regulatory domain contains leucine zipper (LZ), autoinhibitory (AI), and cyclic nucleotide binding (CNB-A and CNB-B) subdomains. **B** and **C**, kinase assays were performed using purified PKG1 $\alpha$  and PKG1 $\beta$  as described in Experimental procedures. Reactions were stopped after 1.5 min (**B**) or 5 min (**C**). Data are from three independent protein preparations, with each point representing the average of three kinase reactions for each preparation. Bars show means  $\pm$  S.D.,  $n = 3$ .

found that the mutant enzyme adopts an active conformation in the absence of cGMP that resembles the conformation of the cGMP-bound WT enzyme.

## Results

### PKG1 $\alpha$ R177Q and PKG1 $\beta$ R192Q kinase activity *in vitro*

We originally found that PKG1 $\alpha$  with an R177Q mutation (RQ-PKG1 $\alpha$ ) caused the kinase to be 90–95% active in the absence of cGMP (14). PKG1 $\beta$  is produced as a splice variant from the same gene, but despite having the same CNB-A and CNB-B domains as PKG1 $\alpha$ , the amount of cGMP required to half-maximally activate PKG1 $\beta$  is  $\sim$ 3.5-fold higher than that of PKG1 $\alpha$  (11). Because the RQ mutation is in CNB-A, we checked to see how the mutation affected PKG1 $\beta$  activity. The N terminus of PKG1 $\beta$  is 15 amino acids longer than that of

PKG1 $\alpha$ , and R192Q PKG1 $\beta$  (RQ-PKG1 $\beta$ ) is directly analogous to RQ-PKG1 $\alpha$  (Fig. 1A). We found that both RQ-PKG1 $\alpha$  and RQ-PKG1 $\beta$  had high basal activities compared with those of the WT enzymes (Fig. 1B), but the basal activity of RQ-PKG1 $\beta$  was consistently higher than that of RQ-PKG1 $\alpha$  ( $88.4\% \pm 5.3\%$  versus  $57.5\% \pm 8.5\%$  of maximal activity in the presence of cGMP). The basal activity of RQ-PKG1 $\alpha$  was lower than we previously reported (14). In our previous study, we measured kinase activity at 10-min time points versus 1.5 min for the assays shown in Fig. 1B (under the conditions used, the assays are linear up to 11 min). At longer time points, activity might be partially driven by PKG1 autophosphorylation (shown below), because autophosphorylation can increase basal kinase activity in the absence of cGMP (12, 16, 17). At a 5-min time point, basal RQ-PKG1 $\beta$  activity reached  $97.8\% \pm 6.1\%$  versus  $75.8\% \pm 20\%$  of maximal activity for RQ-PKG1 $\alpha$  (Fig. 1C). Thus, at longer time points, there is an apparent increase in basal activity in the RQ mutants, which may be driven by autophosphorylation.

### Higher autophosphorylation of RQ-PKG1 *in vitro* but not in cells

We next compared autophosphorylation of WT and mutant kinases. Autophosphorylation of S<sup>65</sup> in PKG1 $\alpha$  and S<sup>80</sup> in PKG1 $\beta$  leads to cGMP-independent kinase activation *in vitro* (12, 16, 17). First, we examined the ability of WT and mutant PKG1 $\alpha$  and PKG1 $\beta$  to autophosphorylate *in vitro*. Purified kinases were incubated in the same buffer used for kinase assays (without peptide substrate) in the presence and absence of 10  $\mu$ M cGMP, and phosphate incorporation was analyzed by SDS-PAGE/autoradiography. We found that RQ-PKG1 $\alpha$  and RQ-PKG1 $\beta$  had higher rates of autophosphorylation than the respective WT enzymes (Fig. 2A and B). It should be noted that the amount of <sup>32</sup>P<sub>o</sub><sub>4</sub> incorporation by autophosphorylation cannot be directly compared between PKG1 $\alpha$  and PKG1 $\beta$ , as <sup>32</sup>P<sub>o</sub><sub>4</sub>- $\gamma$ -ATP-specific activity differed between reactions. Second, to determine whether differential autophosphorylation occurred in cells, we incubated transiently transfected 293T cells with [<sup>32</sup>P]orthophosphate, and some cells were treated with a final concentration of 250  $\mu$ M 8-(4-chlorophenylthio)guanosine-3'-5'-cyclic monophosphate (8-pCPT-cGMP), as indicated. The kinases were isolated under the same conditions used when purifying them for *in vitro* assays, and <sup>32</sup>P<sub>o</sub><sub>4</sub> incorporation was analyzed by SDS-PAGE/autoradiography. We found equivalent amounts of <sup>32</sup>P<sub>o</sub><sub>4</sub> incorporated in the WT and mutant enzymes (Fig. 2C and D), indicating the mutant kinases were not purified in a more highly autophosphorylated state. The observed <sup>32</sup>P<sub>o</sub><sub>4</sub> incorporation likely represents phosphorylation of the activation loop in the catalytic domain, which is necessary for catalytic activity (18). Again, the amount of <sup>32</sup>P<sub>o</sub><sub>4</sub> incorporation into PKG1 $\alpha$  versus PKG1 $\beta$  cannot be directly compared, as experiments were performed at separate times.

### Phosphorylation of VASP in intact cells

We next compared WT and RQ mutant kinase activity in intact cells, using vasodilator-stimulated phosphoprotein

## Characterization of TAAD-associated PKG1

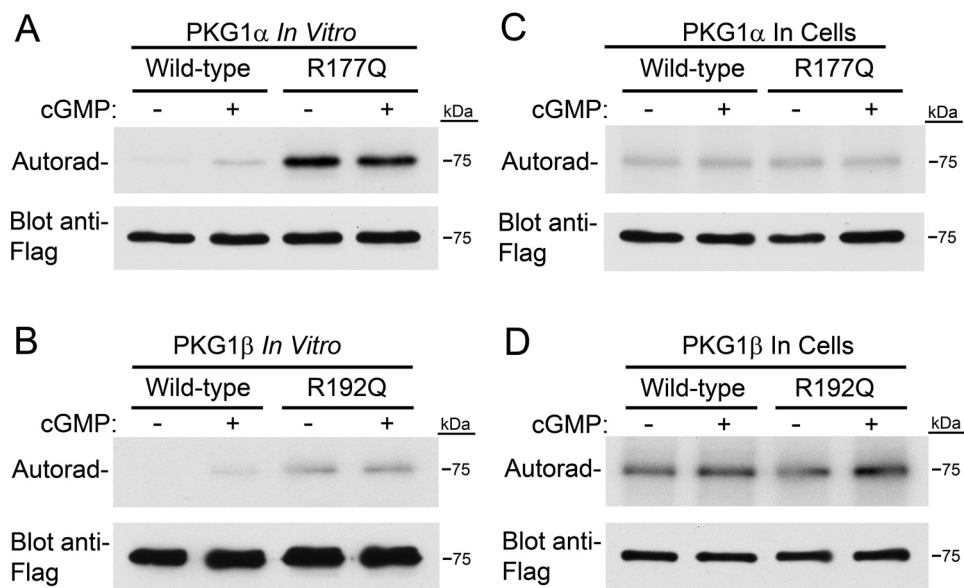


**Figure 2. The RQ mutation causes higher autophosphorylation *in vitro* but not in cells.** *A*, *in vitro* PKG1 $\alpha$  autophosphorylation. Purified PKG1 $\alpha$  was incubated for 5 min with  $^{32}\text{PO}_4\text{-}\gamma\text{-ATP}$  under reaction conditions identical to those used for *in vitro* kinase assays (in the absence of peptide substrate). Phosphate incorporation was determined by SDS-PAGE/autoradiography. Equal loading of the kinase is shown by Western blotting with an anti-Flag antibody. *B*, performed as in panel *A*, except using purified PKG1 $\beta$ . *C*, 293T cells were transfected with expression vectors for Flag-tagged WT and R177Q PKG1 $\alpha$ . Six hours posttransfection, cells were incubated with  $^{32}\text{PO}_4$  for three hours, and then some cells were treated with 8-pCPT-cGMP for one hour. *Upper*, PKG was isolated by anti-FLAG immunoprecipitation, and phosphate incorporation was analyzed by SDS-PAGE/autoradiography. *Lower*, equal PKG amounts were determined by anti-Flag Western blots. *D*, autophosphorylation of PKG1 $\beta$  in 293T cells performed as in panel *C*.

(VASP) phosphorylation as a readout (19). We cotransfected 293T cells with expression vectors for Myc-tagged VASP and WT or RQ-PKG1 $\alpha$  or RQ-PKG1 $\beta$ , and 24 h posttransfection, some wells were treated with a final concentration of 100  $\mu\text{M}$  8-pCPT-cGMP for one hour. VASP phosphorylation was determined by SDS-PAGE/immunoblotting to detect a gel shift induced by Ser<sup>239</sup> phosphorylation (20). 8-pCPT-cGMP treatment of cells transfected with WT PKG1 $\alpha$  caused a complete upward shift in VASP migration (Fig. 3*A*, compare lanes 3 and 4). However, in cells transfected with RQ-PKG1 $\alpha$ , most VASP migrated at the shifted position in the absence of cGMP (Fig. 3*A*, compare lanes 3 and 5), and no further change in migration occurred after treatment with 8-pCPT-cGMP (Fig. 3*A*, compare lanes 5 and 6). Similar results were obtained when VASP was cotransfected with WT and RQ-PKG1 $\beta$  (Fig. 3*B*). Thus, the RQ-PKGs had an increased basal activity in cells under conditions where autophosphorylation did not differ from that of the WT enzymes (Fig. 2*C* and *D*).

### Effect of interchain interactions on RQ mutant activity

In the initial report describing RQ-PKG1 $\alpha$ , we observed that in WT/RQ heterodimers, the WT chain appeared to inhibit the activity of the mutant chain (14). This observation was based on the assumption that equal transfection of WT and mutant Flag-tagged constructs would produce a combination of WT/WT, WT/RQ, and RQ/RQ dimers in a proportion of 1:2:1; however, the exact proportion of each dimer in the preparations was not known. To more carefully assess the role of interchain contacts in regulating RQ-PKG activity, we developed a novel experimental approach using a kinase-dead PKG. In this method, Flag-tagged dead PKG is used to purify active, untagged PKG (Fig. 4*A*). Under these conditions, the Flag-puri-

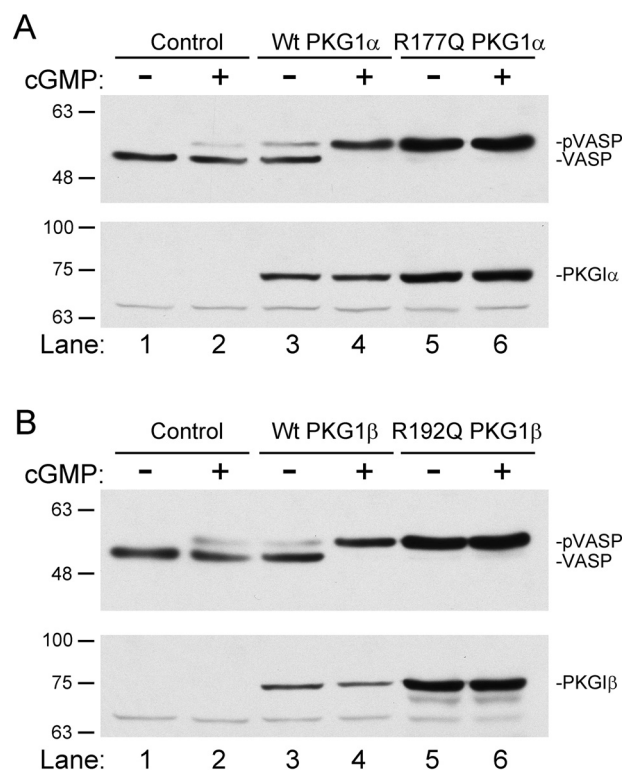


**Figure 3. The RQ mutation increases PKG kinase activity in intact cells.** *A*, 293T cells were cotransfected with expression vectors for Myc-tagged VASP and either WT or R177Q PKG1 $\alpha$ . At 24 h posttransfection, some cells were treated with 100  $\mu\text{M}$  8-pCPT-cGMP for one hour. Cell lysates were analyzed by SDS-PAGE/immunoblotting using antibodies recognizing Myc-epitope (*upper*) or PKG1 (*lower*). *B*, experiment was performed as in panel *A*, but VASP was cotransfected with WT or R192Q PKG1 $\beta$ . The gel shift of VASP indicates S<sup>239</sup> phosphorylation.

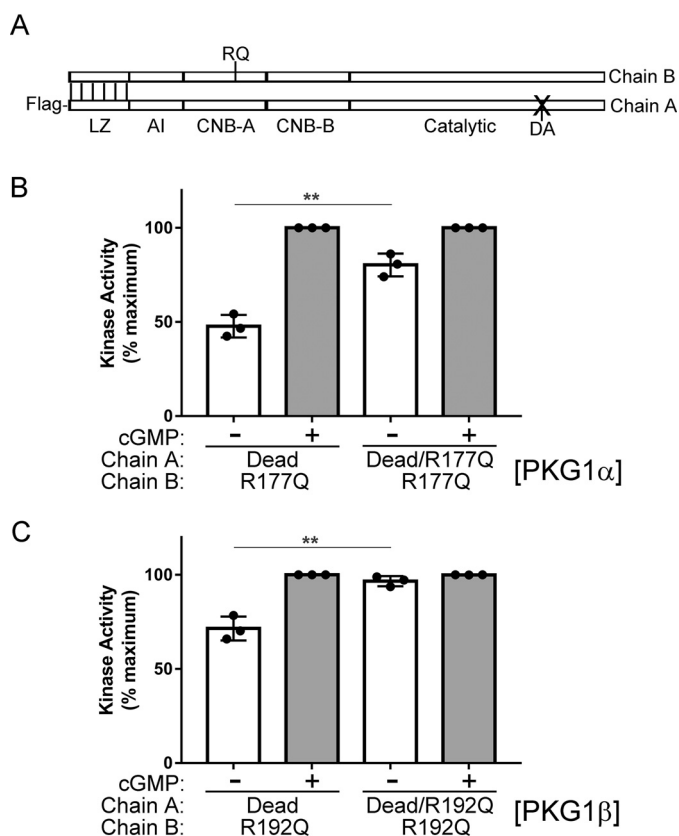


**Figure 4. Interchain communication regulates RQ-PKG1 activity.** A, PKG1 domain map showing dimerized active and dead PKG chains. RQ indicates the site of the activating mutation in CNB-A, and DA indicates mutation of the catalytic aspartic acid to alanine, which causes a loss of kinase activity. B and C, 293T cells were cotransfected with Flag-tagged dead PKG1, with or without the RQ mutation, and untagged active RQ-mutant PKG1. *In vitro* kinase reactions were stopped at 1.5 min to measure the activity of untagged PKG1 $\alpha$  R177Q (B) or PKG1 $\beta$  R192Q (C). Data are from three independent protein preparations, with each point representing the average from three kinase reactions for each preparation. Bars show means  $\pm$  S.D.,  $n = 3$ . \*\*,  $p > 0.01$  by two-tailed Student's *t* test.

fied kinase is a mixture of inactive dead/dead homodimers and dead/active heterodimers. Importantly, the kinase activity measured is that of active chains dimerized to Flag-tagged dead chains. This approach enabled us to compare the effect of the Flag-tagged dead chain, with or without the RQ mutation, on the activity of the untagged, active chain (interchain effect) without having to account for how the mutation affects the activity of its own kinase domain (intrachain effect). We found that basal kinase activity for both RQ-PKG1 $\alpha$  and RQ-PKG1 $\beta$  was lower when the dead chain contained WT CNB-A than with a dead chain with RQ mutant CNB-A (Fig. 4B and C). For PKG1 $\alpha$ , basal activity increased from 44.5 to 77.4% of cGMP-stimulated maximal activity when the dead chain contained the RQ mutation *versus* no CNB-A mutation. For PKG1 $\beta$ , the activity increased from 72.2 to 96.4%. These results clearly demonstrate that the two chains do not act independently and highlight a critical role that interchain contacts play in mediating PKG1 activity. These results also suggest that in humans carrying one copy of the mutant *PRKG1* gene, the pathological consequences of the mutation are most likely reduced by expression of functionally normal PKG1 from the WT gene.

### Effects of cyclic nucleotide analog inhibitors on RQ PKG1 activity

We have recently shown that RQ-PKG1 basal activity can be inhibited by the small peptide inhibitor DT-2, which targets the catalytic cleft (15). Because the RQ mutation is within CNB-A of the regulatory domain, we tested whether cyclic nucleotide analog inhibitors could reduce basal activity of the mutant enzymes. We found that 8-(4-chlorophenylthio)guanosine-3'5'-cyclic monophosphorothioate, Rp-isomer (Rp-8-pCPT-cGMPS), showed a slight agonist activity toward RQ-PKG1 $\alpha$  but had a negligible effect on RQ-PKG1 $\beta$  (Fig. 5A and B). The drug did not inhibit the activity of either kinase at concentrations of up to 300  $\mu$ M. 8-(4-Chlorophenylthio)- $\beta$ -phenyl-1, N<sup>2</sup>-ethenoguanosine-3'5'-cyclic monophosphorothioate, Rp-isomer (Rp-8-pCPT-PET-cGMPS), showed partial agonist activity toward both RQ-PKG1 $\alpha$  and RQ-PKG1 $\beta$ , but at concentrations of  $\geq 100$   $\mu$ M, it inhibited basal activity of both mutant enzymes (Fig. 5C and D). Interestingly, we found that Rp-8-pCPT-PET-cGMPS also inhibited the isolated PKG1 catalytic domain (Fig. 5E), indicating that the inhibition seen in the full-length kinases was not because of binding within the cyclic nucleotide binding pockets. We conclude that the cyclic nucleotide-based inhibitors do not inhibit RQ mutant PKG1 $\alpha$ / $\beta$  basal activity by binding to CNB-A or -B.

### Effect of alternate amino acid substitutions at R<sup>177</sup> on basal kinase activity of PKG1 $\alpha$

At the present time, there are no published crystal structures for PKG1 in the inhibited state. However, there are a number of structures for the closely related cAMP-dependent protein kinase (PKA) in the inhibited state. Using the PKA RI $\alpha$ /C $\alpha$  holoenzyme crystal structure (PDB entry 2QCS) as a template, we used SWISS-Modeler to build a model of inactive PKG1 $\alpha$  (21). Examination of the model shows that Arg<sup>177</sup> makes a number of contacts with remote, nonsequential residues located in CNB-A (Fig. 6A). The Arg<sup>177</sup> hydrophobic arm appears to pack between the side chain of Ile<sup>131</sup> and the backbone region of Gly<sup>137</sup>. These residues are conserved in PKA RI $\alpha$ , suggesting that hydrophobic packing interactions play a general role in stabilizing the inactive state of PKG and PKA. In addition, the charged guanido group of Arg<sup>177</sup> appears to be neutralized by interactions with the backbone carbonyl groups of Leu<sup>139</sup> and Gly<sup>167</sup>.

Next, we used the DUET server to predict the degree to which different R177 mutations would destabilize interactions with contact residues and disrupt the ability of PKG1 to adopt an inhibited conformation (22). The DUET server combines the approaches of two previous *in silico* prediction algorithms (mCSM and SDM) to more accurately predict the destabilizing effect of mutations on proteins (23, 24). For example, we chose alanine because it should not produce novel contacts but would lose the hydrophobic interactions with Ile<sup>131</sup> and Gly<sup>137</sup> and the polar contacts with the Leu<sup>139</sup> and Gly<sup>167</sup> backbone carbonyl groups. DUET predicted that Met would be less and Gln more destabilizing than Ala at position 177 (Fig. 6B). From the structure shown in Fig. 6A, it is evident that replacing Arg<sup>177</sup> with Gln would place Gln's polar side chain (specifically the

## Characterization of TAAD-associated PKG1

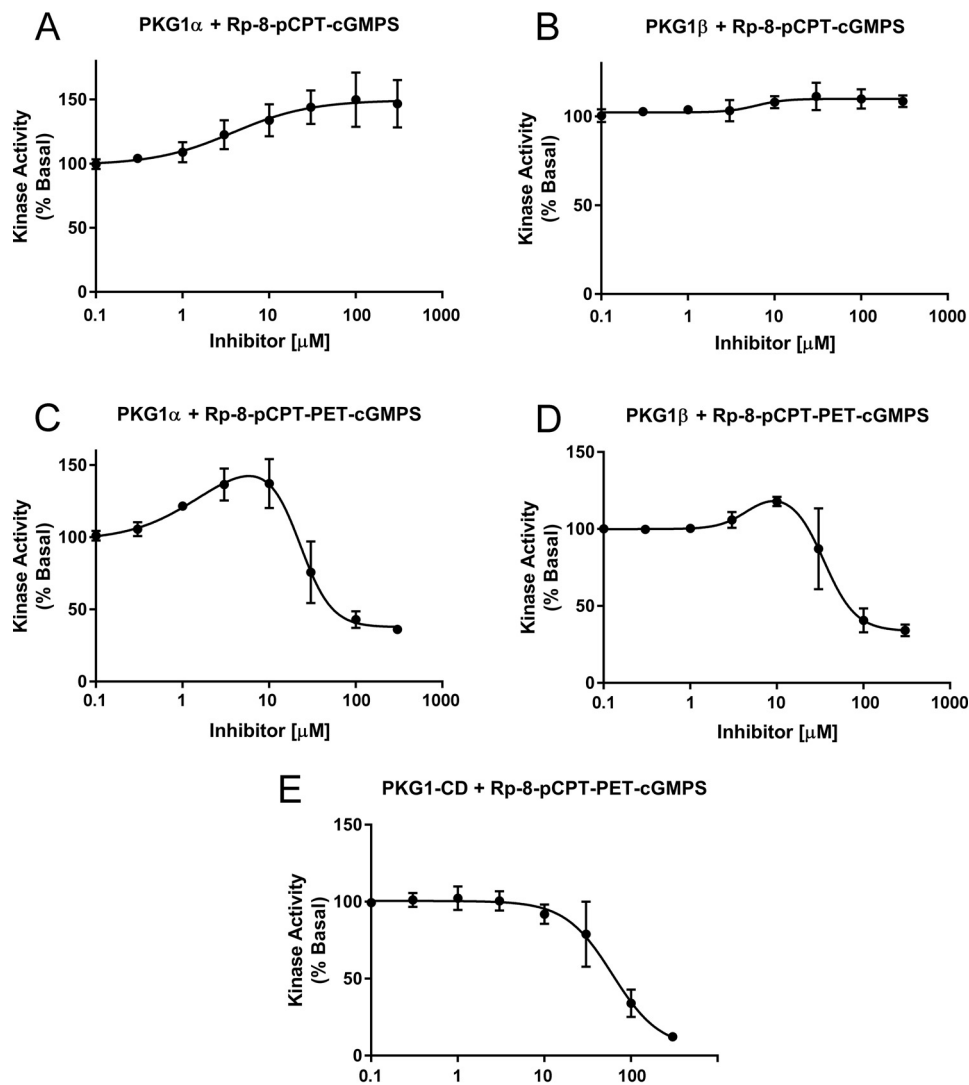


**Figure 5. Effects of cyclic nucleotide analog inhibitors on RQ PKG1 activity.** *In vitro* basal kinase activity of purified R177Q PKG1 $\alpha$  or R192Q PKG1 $\beta$  measured in the presence of increasing concentrations of Rp-8-pCPT-cGMPS (A and B) or Rp-8-pCPT-PET-cGMPS (C and D). E, *In vitro* kinase activity of isolated PKG1 catalytic domain (CD) measured in the presence of increasing Rp-8-pCPT-PET-cGMPS concentrations. For all reactions, basal activity in the absence of inhibitor was set at 100%. Data are the average from three experiments using three independent protein preparations. Bars show means  $\pm$  S.D.,  $n = 3$ .

carboxyl group) in the hydrophobic environment that normally packs around the third methylene group in Arg<sup>177</sup>'s hydrophobic arm.

We tested how the three mutations affect PKG1 $\alpha$  activity *in vitro* and found that all of these substitutions caused an increase in basal activity compared with WT enzyme (Fig. 6C). Each reaction is normalized to the maximum activity seen in the presence of 10  $\mu$ M cGMP in a 1.5-min reaction to minimize autophosphorylation effects. When comparing our assay results to the predicted destabilizing effects of the mutants, we found that, as predicted, Gln was the most destabilizing; however, contrary to DUET analysis, Met was twice as effective as Ala in increasing basal activity.

### Deuterium exchange analysis shows that RQ-PKG1 $\beta$ is in an active conformation

To probe how the RQ mutation affects the conformation of PKG1, we performed H/DX-MS on WT and RQ mutant

PKG1 $\beta$ . Aliquots of purified proteins were incubated with or without cGMP and subsequently incubated with buffered D<sub>2</sub>O. At specific time points, H/D exchange was stopped by adding ice-cold acidic quench buffer. Incorporated deuterons were localized by proteolysis, HPLC fractionation of peptides, and MS. The H/D exchange data were then analyzed with respect to a PKG1 $\beta$  structural model (Fig. 7A and B).

We first examined peptides within the regulatory domain (Fig. 7B, shown in yellow and teal, starting with the autoinhibitory loop, AI). The addition of cGMP to WT PKG1 $\beta$  caused increased solvent exposure in a peptide comprising the autoinhibitory loop (residues 69–86, shown in yellow); however, in RQ-PKG1 $\beta$ , even in the absence of cGMP this peptide had levels of deuterium incorporation equal to that of the WT in the presence of cGMP, and H/D exchange was not increased in the presence of cGMP (Fig. 7C). In contrast to the autoinhibitory loop peptide, deuterium incorporation in a peptide (aa 59–68) just N terminal to the autoinhibitory loop showed identical H/D exchange behavior between WT and mutant PKG, and

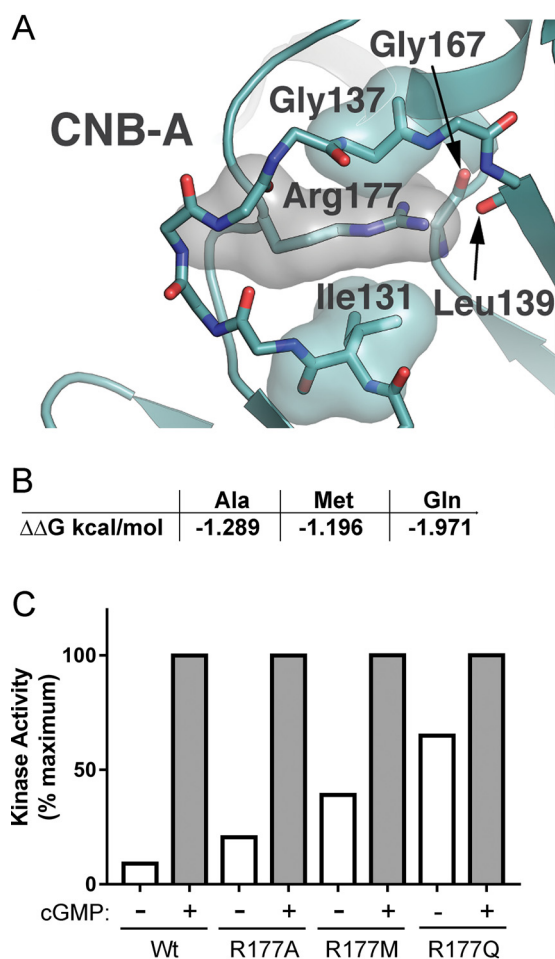


**Figure 6. Mutation of R177 to Ala, Met, or Gln leads to increased basal kinase activity.** *A*, molecular model of inactive PKG1 $\alpha$  showing putative packing of PKG $\alpha$  R177 in an inactive conformation. *B*, *in silico*-predicted destabilizing effects of mutations at R177 using the DUET server ( $\Delta\Delta G$  in kcal/mol). *C*, kinase assays comparing basal to maximum cGMP-stimulated activation of WT and mutant PKG1 $\alpha$ . Data are from triplicate reactions from a single protein preparation. The experiment was performed twice with similar results.

cGMP had no effect (Fig. 7D). In addition, a peptide (aa 93–111) just C terminal to the loop binding the catalytic cleft showed a trend toward higher H/D exchange in mutant PKG1 $\beta$ , but H/D exchange was not altered by cGMP in either the WT or mutant protein (Fig. 7E). Thus, cGMP induces increased solvent exposure of the autoinhibitory loop in WT PKG1 $\beta$ , but the autoinhibitory loop of RQ-PKG1 $\beta$  shows high solvent exposure even in the absence of cGMP, and exposure is not further increased in the presence of cGMP.

Next, we examined peptides in the catalytic domain (Fig. 8, shown in gray). Alverdi *et al.* have previously used H/D exchange to examine cGMP-induced conformational changes in PKG1 $\alpha$  and observed that cGMP caused increased H/D exchange within peptides flanking the catalytic cleft (13). We found a similar phenomenon in WT PKG1 $\beta$ ; in the presence of cGMP, H/D exchange increased in peptides comprising amino acids 521–533 (shown in green), 547–556 (shown in red), and 565–583 (shown in blue), all of which flank the catalytic cleft (Fig. 8). However, in RQ-PKG1 $\beta$ , in the absence of cGMP, H/D exchange within these peptides resembled H/D exchange in the

WT enzyme in the presence of cGMP, and H/D exchange of the mutant enzyme did not increase when cGMP was added. Taken together, our data demonstrate that the RQ mutation causes PKG1 to adopt an active conformation in the absence of cGMP, similar to the WT, cGMP-bound kinase.

## Discussion

In this study, we probed how the RQ-PKG1 mutation associated with familial thoracic aortic aneurysms and aortic dissections leads to increased basal kinase activity. In the original report describing mutant PKG1 $\alpha$ , we were surprised to find that the mutation led to increased basal activity with normal cGMP-stimulated maximal activity, as the mutation disrupted cGMP binding to CNB-A (14). In our current study, we found that the mutation also increased basal activity of PKG1 $\beta$ . In fact, the mutation appeared to increase basal activity of RQ-PKG1 $\beta$  more than that of RQ-PKG1 $\alpha$ . This difference is most likely driven by the unique N termini, which cause isoform-specific cGMP affinities and activation constants (25, 26).

De Jong *et al.* first reported PKG1 autophosphorylation in 1977 (27). Subsequently, Aitken *et al.* found that PKG1 $\alpha$  underwent autophosphorylation on multiple sites *in vitro*, and that autophosphorylation at these sites occurred at different rates (16). Notably, whereas phosphorylation of Thr<sup>59</sup> occurs relatively quickly, phosphorylation at Ser<sup>65</sup> is much slower; however, autophosphorylation at Ser<sup>65</sup> leads to cGMP-independent kinase activation, whereas modification of Thr<sup>59</sup> does not (11). Similar results were found for PKG1 $\beta$ , where autophosphorylation of Ser<sup>64</sup> occurs quickly but has no effect on basal kinase activity, and autophosphorylation at Ser<sup>80</sup> occurs slowly, leading to cGMP-independent activity (12).

Although we found that the RQ mutation caused both PKG1 $\alpha$  and PKG1 $\beta$  to have higher rates of autophosphorylation *in vitro* than the WT enzymes (with or without cGMP), we did not detect increased autophosphorylation of mutant PKG in intact cells. The reason why PKG1 $\alpha$  and PKG1 $\beta$  autophosphorylate *in vitro* and not in cells is not known. Preliminary experiments suggest that it is because of the relatively higher amount of Mg<sup>2+</sup> relative to the ATP concentration used in *in vitro* reactions (D. Casteel, unpublished results). In addition, it is unknown why the mutant enzymes undergo more rapid autophosphorylation *in vitro* than the WT enzymes; the mutation may release the enzyme's phosphotransfer activity without reducing the catalytic cleft's access to the autoinhibitory loop (where the autophosphorylation sites are located). Consistent with our results indicating a lack of autophosphorylation in intact cells, Vallur *et al.* could not detect PKG1 $\alpha$ /PKG1 $\beta$  autophosphorylation in a number of cell types using phospho-specific antibodies (28). It has been hypothesized that PKG1 autophosphorylation leads to sustained PKG1 signaling after cellular cGMP levels fall (29); however, our findings, combined with those of Vallur *et al.*, cast doubt on the physiological significance of PKG1 autophosphorylation.

As mentioned, we previously demonstrated that the activity of RQ-PKG1 $\alpha$  could be inhibited by DT-2 *in vitro* (15). Another class of PKG inhibitors consists of modified cGMP analogs in which one of the phosphate oxygen atoms is replaced with

## Characterization of TAAD-associated PKG1

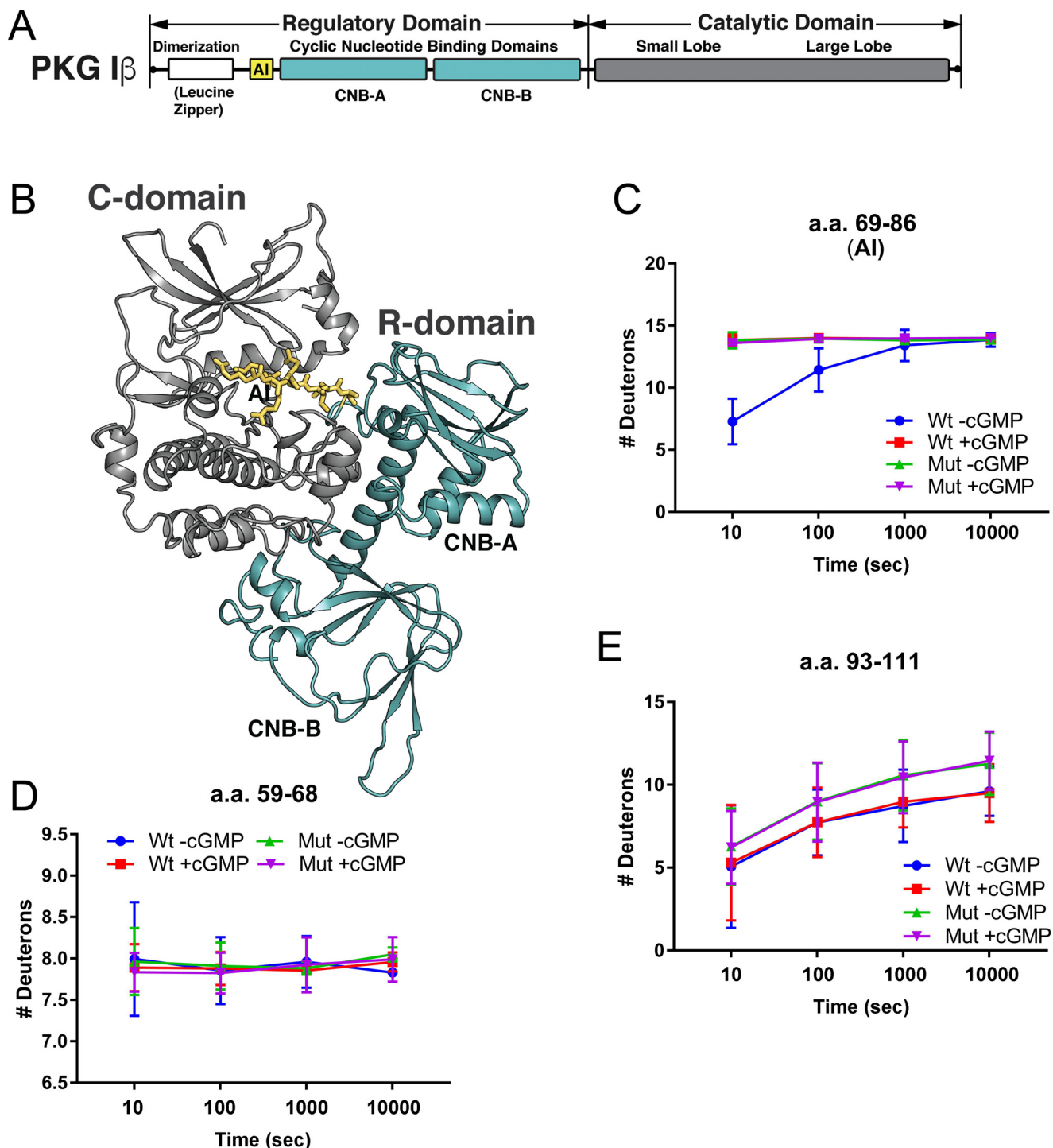


**Figure 7. H/D exchange in inhibitory loop residues.** A, PKG1 $\beta$  domain organization colored according to the molecular model shown in panel B. LZ, leucine zipper; AI, autoinhibitory loop; CNB-A and CNB-B, cyclic nucleotide binding pockets; and catalytic, the catalytic domain. (B) Molecular model of PKG1 $\beta$  in an inhibited conformation with the regulatory domain CNBs colored teal, catalytic domain in gray, and amino acids 69–86 of the linker/autoinhibitory loop colored yellow. (C) Time-dependent H/D exchange in residues 69–86 (AI), which bind within the catalytic cleft. (D) Time-dependent H/D exchange in residues 59–68, which are N terminal to the autoinhibitory loop. (E) Time-dependent H/D exchange in residues 93–111, which are C terminal to the autoinhibitory loop. Wt, WT PKG1 $\beta$ ; Mut, R192Q PKG1 $\beta$ . Graphs show the number of deuterons incorporated into the peptides as a function of time. H/D exchange data are averages from two independent H/D exchange reactions performed with two separate protein preparations.

sulfur, *i.e.* Rp-phosphorothioate cGMP analogs (30). These inhibitors bind within the cGMP-binding pockets and prevent activation of WT enzyme by blocking cGMP access. We tested two of these inhibitors for their ability to inhibit RQ-PKG1 $\alpha$  and RQ-PKG1 $\beta$  and found that both inhibitors showed partial

agonist activity toward the mutant kinases. Our findings are consistent with partial agonist activities of various Rp-phosphorothioate cGMP analogs seen by others with WT PKG1 $\alpha$  (31, 32). Interestingly, at higher concentrations, Rp-pCPT-PET-cGMPS inhibited both RQ-PKG1 $\alpha$  and RQ-PKG1 $\beta$ , but



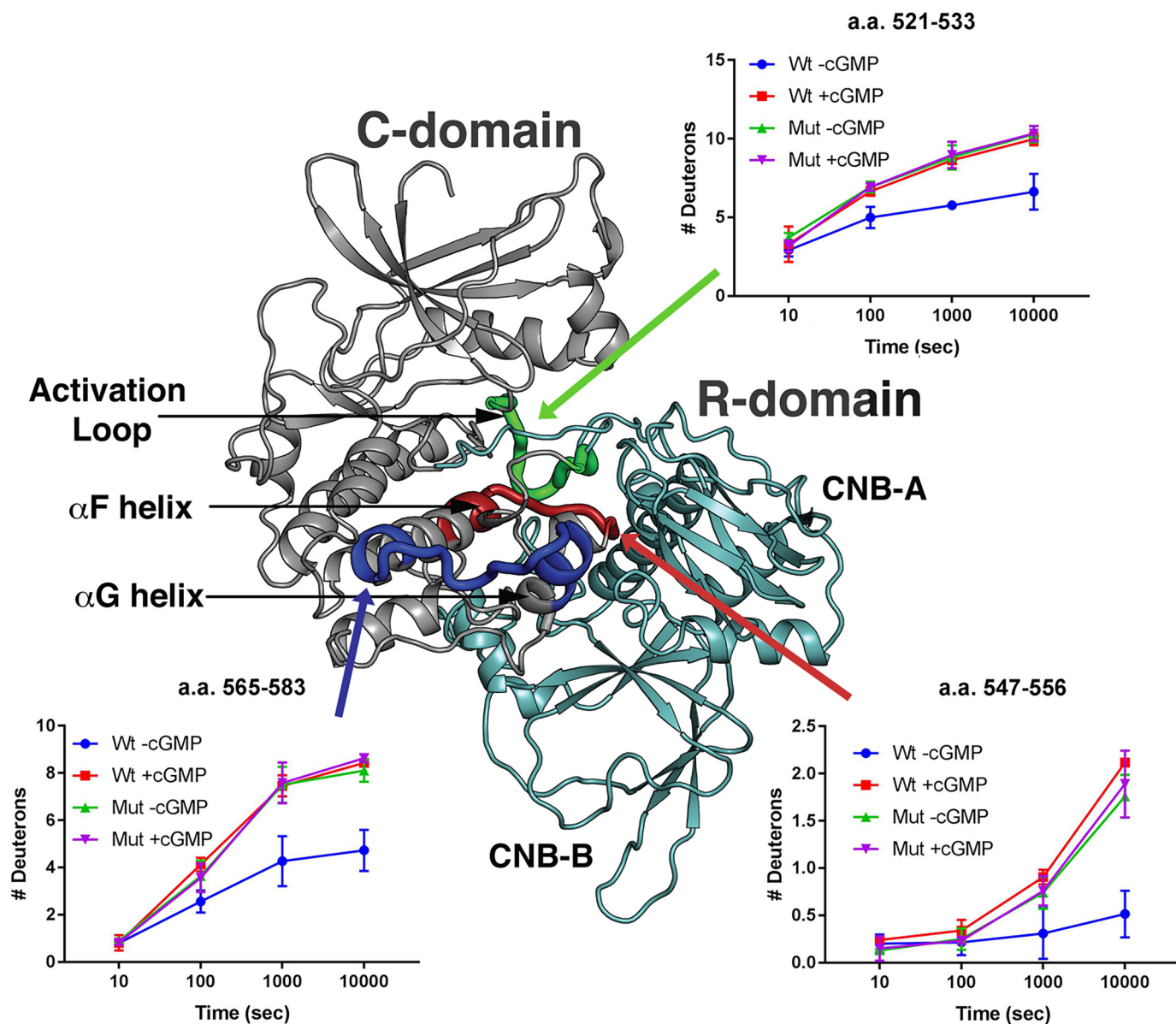


**Figure 8.** H/D exchange in the catalytic cleft of WT and R192Q PKG1 $\beta$ . H/D exchange profiles of peptides from WT (Wt) and R192Q (Mut) PKG1 $\beta$  in the presence or absence of cGMP are shown mapped to a molecular model of inactive PKG1 $\beta$ . The regulatory domain is colored teal and the catalytic domain is mainly colored gray, with the following exceptions: the region containing amino acids 521–533 is colored green; 547–556 is colored red; and 565–583 is colored dark blue. Graphs show the number of deuterons incorporated into the peptides as a function of time. H/D exchange data are the averages from two independent H/D exchange reactions performed with separate protein preparations.

we found that it also inhibited the isolated PKG1 catalytic domain. Whereas the exact mechanism of inhibition of the catalytic domain remains unknown, it is possible that Rp-pCPT-PET-cGMPs acts as an ATP analog inhibitor.

We used a novel method to demonstrate the role of interchain communication in modulating activity of the mutant kinase. In WT/RQ heterodimers, the activity of the mutant chain is clearly inhibited by the WT chain. How interchain interactions control PKG1 activity has not been thoroughly studied; however, two reports have provided some preliminary insights. Based on the crystal structure of PKG1 $\alpha$ 's cyclic nucleotide binding pockets, Osborne *et al.* identified a hydrophobic interface that formed between the two chains of a PKG1 dimer (33). When the hydrophobic residues (and a neighboring aspara-

gine) were mutated to alanines, the basal activity of the kinase increased, suggesting that the interchain interaction stabilized the inactive conformation of the enzyme (33). In another study, Kim *et al.* identified a cGMP-mediated interface between the two chains that maintained the kinase in the active conformation (34). Consistent with this, when N<sup>189</sup> in the interface was changed to alanine, the activation constant ( $K_a$ ) for cGMP in full-length/dimeric PKG1 $\beta$  increased from 140 nM to 2.5  $\mu$ M, whereas the mutations had only a slight effect on the  $K_a$  for cGMP in truncated/monomeric PKG1 $\beta$ . It should be noted that the  $K_a$  for cGMP was already increased in the truncated PKG1 $\beta$  (1.5  $\mu$ M); thus, the effect of the interface mutation might have been masked by an apparently decreased cGMP affinity in the monomeric enzyme. The new method described in

## Characterization of TAAD-associated PKG1

this work should be useful in further studies examining how interchain communication regulates PKG1 activity.

Our H/D exchange analysis demonstrated that the RQ mutation causes PKG1 $\beta$  to adopt a conformation that resembles the active cGMP-bound WT protein, even in the absence of cGMP. Specifically, in WT PKG1 $\beta$  we observed increased H/D exchange in peptides comprising the autoinhibitory loop and the catalytic cleft in the presence, compared with the absence, of cGMP. In the mutant enzyme, in the absence of cGMP, the autoinhibitory loop and catalytic cleft peptides showed H/D exchange behavior that mirrored H/D exchange in cGMP-bound WT, and adding cGMP did not lead to a further increase in H/D exchange. This result was a bit surprising, because RQ-PKG1 $\beta$  is not 100% active (*i.e.* it can still be stimulated by cGMP). However, RQ-PKG1 $\beta$  is 88% active and the H/D exchange analysis may not be sensitive enough to detect a 10–12% increase in deuteration upon cGMP binding. In addition, PKG1 $\beta$ 's inhibited conformation may be stabilized by Mg<sup>2+</sup>/ATP, which is present in the kinase assays but not in the H/D exchange reactions. In PKA, the affinity between RI $\alpha$ /regulatory and C $\alpha$ /catalytic subunits is 125 nM in the absence of Mg<sup>2+</sup>/ATP, but the affinity decreases to <0.05 nM in the presence of Mg<sup>2+</sup>/ATP (35). It would be interesting to perform H/D exchange experiments on full-length WT and RQ mutant PKG in the presence of Mg<sup>2+</sup> and a nonhydrolyzable ATP analog to see if these ligands partially stabilize the inactive conformation and decrease H/D exchange in peptides within the autoinhibitory loop and catalytic cleft.

In conclusion, using H/D exchange MS, we found that the RQ mutation causes PKG1 $\beta$  to adopt an active conformation in the absence of cGMP. A dynamic equilibrium exists between inactive and active conformations of PKG1, and cyclic nucleotide binding normally stabilizes an active conformation of the WT enzyme, as previously discussed for PKA (36). Because mutations other than RQ at position 177 of PKG1 $\alpha$  also led to activation, the mechanism does not appear to involve glutamine making unique contacts that stabilize an active conformation; rather, activation results from the destabilization of an inactive conformation. In comparison, single-amino-acid substitutions in small RAS GTPases and G protein-coupled receptors also lead to constitutive activity by shifting the proteins' conformation to an active state (37–39). Whereas high levels of RQ-PKG1 autophosphorylation might drive some of the increased activity seen *in vitro*, autophosphorylation does not appear to occur in cells and, thus, does not contribute to increased signaling of the mutant kinase *in vivo*. The fact that the inactive WT chain in WT/RQ heterodimers reduces the activity of the mutant chain suggests that interventions reducing cGMP levels in patients carrying RQ mutant PKG1 reduces the pathological effects of the mutation.

## Experimental procedures

### Materials

Anti-Flag affinity gel, anti-Flag M2 antibodies, and Flag peptide were from Sigma. Monoclonal mouse anti-Myc-epitope antibody was from Santa Cruz Biotechnology. Horseradish peroxidase-conjugated goat anti-mouse antibodies were from

Jackson ImmunoResearch Laboratories. Kemptide was from Anaspec. Radioisotopes were from Perkin Elmer. Protease inhibitor mixture was from Calbiochem. Cell culture medium was from Cellgro, and fetal bovine serum was from Cellgro and Atlanta Biologicals. Tissue culture plates were from Fisher Scientific. KOD Hot Start DNA polymerase was from Novagen. Restriction enzymes and T4 DNA ligase were from New England Biolabs. Lipofectamine 2000 was from Life Technologies. 8-pCPT–cGMP, Rp-8-pCPT–cGMPs, and Rp-8-pCPT–PET–cGMPs were from Biolog. General supplies and chemicals were from Sigma and Fisher Scientific.

### Expression plasmids

Flag-tagged expression constructs for PKG1 $\alpha$ , PKG1 $\beta$ , PKG1 $\beta$ -CD, and RQ-PKG1 $\alpha$  have been described previously (14, 40). RQ-PKG1 $\beta$  was created by swapping the PKG1 $\beta$  N terminus for the PKG1 $\alpha$  N terminus in the mutant construct using an internal NcoI site. Myc-tagged human VASP was constructed by PCR using VSV-tagged VASP as a template (41) with the following primers: 5'-GCTGAATTCGCCGC-CATGGCTGCCATCCGGAAGAAAC-3' (sense) and 5'-GCT-CTCGAGTCACAAGACAAGGCACCC-3' (antisense). The PCR product was digested with EcoRI and XhoI and ligated into a vector that put an in-frame Myc tag at the N terminus. Additional PKG1 $\alpha$  mutations were generated by overlapping extension PCR using high-fidelity KOD Hot Start DNA polymerase (42). All constructs that underwent a PCR step were sequenced to ensure the presence of the desired mutation and the absence of PCR-generated errors.

### Protein expression and purification

For kinase assays, 293T cells were plated into 6-well cluster dishes such that they were 90–95% confluent the next day. For each protein preparation, three wells were transfected with 2  $\mu$ g Flag-tagged expression construct per well using Lipofectamine 2000. The next day (16–20 h later), cells were scraped in PBS (10 mM Na<sub>2</sub>HPO<sub>4</sub>, 2 mM KH<sub>2</sub>PO<sub>4</sub>, 137 mM NaCl, 2.7 mM KCl, pH 7.4), pelleted by centrifugation, and snap frozen in a dry ice-ethanol bath. The pellets were stored at –80°C until needed. Cells were lysed in 400  $\mu$ l ice-cold buffer A (PBS, 0.1% NP-40) with 1 $\times$  protease inhibitor mixture (Calbiochem), and lysates were cleared by centrifugation (16,000  $\times$  g, 10 min at 4°C). Cleared lysates were incubated with 20  $\mu$ l anti-Flag affinity gel for one hour at 4°C with constant mixing. Beads were washed twice with 200  $\mu$ l buffer A, twice with 200  $\mu$ l PBS containing a total of 500 mM NaCl, and twice with 200  $\mu$ l PBS. Bound protein was eluted by incubating the beads 4 times with 10  $\mu$ l elution buffer (PBS with 100  $\mu$ g/ml Flag peptide). For each elution step, the beads were incubated with buffer for 5 min on ice. The four eluates for each protein were pooled.

For H/DX-MS analysis, 293T cells were plated into eight 10-cm tissue culture dishes, and the next day four dishes each were transfected with 12  $\mu$ g Flag-tagged expression construct encoding WT or RQ PKG1 $\beta$  using Lipofectamine 2000. Cells were harvested as described above, each pellet was lysed in 400  $\mu$ l ice-cold buffer A (PBS, 0.1% NP-40) with 1 $\times$  protease inhibitor mixture (Calbiochem), and lysates were cleared by

centrifugation ( $16,000 \times g$ , 10 min at  $4^\circ\text{C}$ ). Cleared lysates were incubated with  $80 \mu\text{l}$  anti-Flag affinity gel for one hour at  $4^\circ\text{C}$  with constant mixing. Beads were washed twice with  $500 \mu\text{l}$  buffer A, twice with  $500 \mu\text{l}$  PBS containing a total of  $500 \text{ mM}$  NaCl, and twice with  $500 \mu\text{l}$   $10 \text{ mM}$  Tris (pH 7.2) with  $150 \text{ mM}$  NaCl. Bound proteins were eluted by incubating the beads 4 times with  $40 \mu\text{l}$  elution buffer ( $10 \text{ mM}$  Tris [pH 7.2],  $150 \text{ mM}$  NaCl and  $200 \mu\text{g/ml}$  Flag peptide). For each elution step, the beads were incubated with buffer for 5 min on ice. The four eluates for each protein were pooled and dialyzed overnight at  $4^\circ\text{C}$  in  $10 \text{ mM}$  Tris (pH 7.2),  $150 \text{ mM}$  NaCl. The proteins were concentrated to  $\sim 2 \mu\text{g}/\mu\text{l}$  using a  $10,000$ -molecular-weight-cutoff Microcon device (Millipore).

### Kinase assays

Flag-tagged purified WT and mutant PKG1 proteins were diluted to  $\sim 1 \text{ ng}/\mu\text{l}$  in KPEM buffer ( $10 \text{ mM}$  potassium phosphate [pH 7.0],  $1 \text{ mM}$  EDTA, and  $25 \text{ mM}$  mercaptoethanol) with  $0.1\%$  BSA. To avoid possible oxidation-induced activation of PKG1 $\alpha$ , assays were performed within one hour of purification. Diluted kinase ( $10 \mu\text{l}$ ) was added to  $5 \mu\text{l}$   $3\times$  kinase reaction mix ( $120 \text{ mM}$  HEPES [pH 7.0],  $24 \mu\text{g}$  Kemptide,  $30 \text{ mM}$   $\text{MgCl}_2$ ,  $180 \mu\text{M}$  ATP,  $1.8 \mu\text{Ci}$   $^{32}\text{PO}_4$ - $\gamma$ -ATP) with or without cGMP at a final concentration of  $10 \mu\text{M}$ . In some reactions, the indicated amounts of inhibitors were added to reaction mixes. Reactions were incubated at  $30^\circ\text{C}$  and stopped at 1.5, 2, or 5 min by spotting on P81 phosphocellulose paper. Unincorporated  $^{32}\text{PO}_4$ - $\gamma$ -ATP was removed by washing 4 times in 2 liters of  $0.452\%$  o-phosphoric acid.  $^{32}\text{PO}_4$  incorporation was measured by liquid scintillation counting. Curve fitting for kinase reactions with inhibitors was done by nonparametric analysis using Graphpad Prism. For Rp-8-pCPT-cGMPS, which only showed agonist activity in the full-length RQ mutants, we used log (agonist) *versus* response (stimulation). Because the assays using Rp-8-pCPT-PET-cGMPS with full-length kinases showed a partial agonist and then inhibitory response, we used the bell-shaped curve. Finally, for assays examining the effect of Rp-8-pCPT-cGMPS on PKGI catalytic domain activity, we used log (agonist) *versus* response (inhibition).

### Autophosphorylation assays

For *in vitro* autophosphorylation reactions, purified WT and RQ mutant PKG1 $\alpha$  and PKG1 $\beta$  were incubated under reaction conditions identical to those used for kinases assays, except that Kemptide was omitted. Reaction mixtures were incubated at  $30^\circ\text{C}$  for 1.5 min and were stopped by adding SDS sample buffer. Reactants were separated by SDS-PAGE, and proteins were transferred to Immobilon P. Phosphate incorporation was determined by autoradiography. Equal loading was determined by Western blotting with anti-Flag antibodies.

For autophosphorylation studies in intact cells, 293T cells were seeded into 6-well cluster dishes the day before transfection, such that they would be  $80$ – $90\%$  confluent at the time of transfection. The cells were transfected with expression vectors for Flag-tagged WT and RQ mutant PKG1 $\alpha$  or PKG1 $\beta$  using Lipofectamine 2000 (Life Technologies). Four hours posttransfection, cells were placed in phosphate-free DMEM supple-

mented with  $100 \mu\text{Ci}$  [ $^{32}\text{P}$ ]orthophosphate per well. Three hours later, a final concentration of  $250 \mu\text{M}$  8-pCPT-cGMP (Biolog) was added to the appropriate wells for one hour. The cells were harvested by scraping in buffer A supplemented with  $1\times$  protease inhibitor mixture (Calbiochem). Cleared lysates were incubated with anti-Flag M2 affinity gel (Sigma) for one hour at  $4^\circ\text{C}$ . The beads were washed, and phosphorylation levels in bound proteins were determined by SDS-PAGE/autoradiography.

### Molecular modeling of inactive PKG1 $\beta$

The model of PKG1 $\beta$  in its inactive state was generated using the Swiss Model server (21). Briefly, the primary sequence of PKG1 $\beta$  was used as the input, with the PKA in structure 2QCS used as the template (43). This PKA structure contains the catalytic domain bound by the regulatory domain and represents the inactive conformation, and each PKG1 $\beta$  domain was modeled independently. To create the full model, the server-generated structures were aligned with the PKA regulatory and catalytic chains in 2QCS using PyMol (Schrodinger, LLC).

### Hydrogen/deuterium exchange analysis

Peptide fragment optimization was performed by incubating  $2 \mu\text{g}$  purified WT or RQ-PKG1 $\beta$  in quench buffer containing different final concentrations of guanidium HCl ( $0.5$ ,  $1$ ,  $2$ , and  $4 \text{ M}$ ). We found that  $2 \text{ M}$  guanidium gave the best peptide coverage ( $>90\%$ ). Before performing the H/D exchange reactions, aliquots of WT and RQ-PKG1 $\beta$  were incubated with  $20 \mu\text{M}$  cGMP on ice for 1 h. Exchange reactions were initiated by adding  $30 \mu\text{l}$  PKG to  $90 \mu\text{l}$  buffered  $\text{D}_2\text{O}$  ( $12.5 \text{ mM}$  Tris, pH 7.2, and  $150 \text{ mM}$  NaCl). At the appropriate time points, H/D exchange was terminated by adding  $24 \mu\text{l}$  of the exchange reaction to  $36 \mu\text{l}$  ice-cold quench buffer ( $3.6 \text{ M}$  guanidium HCl,  $0.8\%$  formic acid, and  $16.6\%$  glycerol). Undeuterated samples were prepared by incubating  $6 \mu\text{l}$  PKG for  $10 \text{ s}$  with  $18 \mu\text{l}$  buffered  $\text{H}_2\text{O}$  (as described above), followed by the addition of  $36 \mu\text{l}$  quench buffer. Fully deuterated reference samples were prepared by incubating  $6 \mu\text{l}$  PKG with  $18 \mu\text{l}$   $\text{D}_2\text{O}$ - $0.8\%$  formic acid at room temperature overnight and then adding quench buffer. All samples were split into two  $30$ - $\mu\text{l}$  aliquots, frozen on dry ice, and stored at  $-80^\circ\text{C}$  until analysis by proteolysis/MS. H/D exchange experiments were performed twice using two independent protein preparations for both WT and RQ-PKG1 $\beta$ . Tables S1 and S2 contain H/D exchange data for all of the manually confirmed peptides identified in the first H/DX-MS experiment.

MS, quantification of deuterium incorporation, corrections for back exchange, and data analysis were performed as described previously (44). Briefly, samples were quickly thawed at  $4^\circ\text{C}$ , proteolyzed by passing through a pepsin column, and collected on a  $\text{C}_{18}$  reverse-phase column at  $0^\circ\text{C}$ . Peptides were eluted using a linear gradient of  $0.046\%$  (v/v) TFA,  $6.4\%$  (v/v) acetonitrile to  $0.03\%$  (v/v) TFA, and  $38.4\%$  (v/v) acetonitrile over a  $30$ -min run. Eluted peptides were analyzed using an Orbitrap Elite mass spectrometer (ThermoFisher) and identified using Proteome Discoverer software (ThermoFisher). The centroids of the isotopic envelopes of nondeuterated, time

## Characterization of TAAD-associated PKG1

course-deuterated, and fully deuterated peptides were measured using DXMS Explorer software (Sierra Analytics). Corrections for back exchange were made by measuring deuterium loss in peptides derived from the fully deuterated samples.

### Data availability

All of the relevant data are contained within the article.

**Author contributions**—M. H. C., S. A., T. H., A. T., S. L., and D. E. C. investigation; C. K., R. B. P., and D. E. C. formal analysis; C. K. and D. E. C. visualization; R. B. P. resources; R. B. P. funding acquisition; R. B. P. and D. E. C. writing-review and editing; D. E. C. conceptualization; D. E. C. data curation; D. E. C. supervision; D. E. C. validation; D. E. C. methodology; D. E. C. writing-original draft; D. E. C. project administration.

**Funding and additional information**—This work was supported by the National Institutes of Health grants R01-HL132141 (to R. B. P.), R01-GM090161 (to C. K.), and 1U19AI117905, R01-GM020501 (to S. L.). The content is solely the responsibility of the authors and does not necessarily represent the official views of the National Institutes of Health.

**Conflict of interest**—The authors declare no conflicts of interest with the content of this article.

**Abbreviations**—The abbreviations used are: PKG, protein kinase G; AI, autoinhibitory; H/D, hydrogen-deuterium; H/DX-MS, hydrogen/deuterium exchange MS; Rp-8-pCPT-PET-cGMPS, 8-(4-chlorophenylthio)- $\beta$ -phenyl-1,N<sup>2</sup>-ethenoguanosine-3'5'-cyclic monophosphorothioate, Rp-isomer; 8-pCPT-cGMP, 8-(4-Chlorophenylthio)-guanosine-3'5'-cyclic monophosphate; Rp-8-pCPT-cGMPS, 8-(4-chlorophenylthio)guanosine-3'5'-cyclic monophosphorothioate, Rp-isomer.

### References

- Hofmann, F., Bernhard, D., Lukowski, R., and Weinmeister, P. (2009) cGMP regulated protein kinases (cGK). *Handb. Exp. Pharmacol.* **191**, 137–162 [CrossRef](#)
- Francis, S. H., Busch, J. L., Corbin, J. D., and Sibley, D. (2010) cGMP-dependent protein kinases and cGMP phosphodiesterases in nitric oxide and cGMP action. *Pharmacol. Rev.* **62**, 525–563 [CrossRef Medline](#)
- Friebe, A., Sandner, P., and Schmidtko, A. (2017) Meeting report of the 8th International Conference on cGMP “cGMP: generators, effectors, and therapeutic implications” at Bamberg, Germany, from June 23 to 25, 2017. *Naunyn. Schmiedeberg's Arch. Pharmacol.* **390**, 1177–1188 [CrossRef Medline](#)
- Casteel, D. E., Zhuang, S., Gudi, T., Tang, J., Vuica, M., Desiderio, S., and Pilz, R. B. (2002) cGMP-dependent protein kinase I beta physically and functionally interacts with the transcriptional regulator TFII-I. *J. Biol. Chem.* **277**, 32003–32014 [CrossRef Medline](#)
- Kato, M., Blanton, R., Wang, G. R., Judson, T. J., Abe, Y., Myoishi, M., Karas, R. H., and Mendelsohn, M. E. (2012) Direct binding and regulation of RhoA protein by cyclic GMP-dependent protein kinase Ialpha. *J. Biol. Chem.* **287**, 41342–41351 [CrossRef Medline](#)
- Schlossmann, J., Ammendola, A., Ashman, K., Zong, X., Huber, A., Neubaer, G., Wang, G. X., Allescher, H. D., Korth, M., Wilm, M., Hofmann, F., and Ruth, P. (2000) Regulation of intracellular calcium by a signalling complex of IRAG, IP3 receptor and cGMP kinase Ibeta. *Nature* **404**, 197–201 [CrossRef Medline](#)
- Surks, H. K., Mochizuki, N., Kasai, Y., Georgescu, S. P., Tang, K. M., Ito, M., Lincoln, T. M., and Mendelsohn, M. E. (1999) Regulation of myosin phosphatase by a specific interaction with cGMP-dependent protein kinase Ialpha. *Science* **286**, 1583–1587 [CrossRef Medline](#)
- Tang, K. M., Wang, G.-R., Lu, P., Karas, R. H., Aronovitz, M., Heximer, S. P., Kaltenbronn, K. M., Blumer, K. J., Siderovski, D. P., Zhu, Y., Mendelsohn, M. E., Tang, M., and Wang, G. (2003) Regulator of G-protein signaling-2 mediates vascular smooth muscle relaxation and blood pressure. *Nat. Med.* **9**, 1506–1512 [CrossRef Medline](#)
- Yuasa, K., Michibata, H., Omori, K., and Yanaka, N. (1999) A novel interaction of cGMP-dependent protein kinase I with troponin T. *J. Biol. Chem.* **274**, 37429–37434 [CrossRef Medline](#)
- Yuasa, K., Omori, K., and Yanaka, N. (2000) Binding and phosphorylation of a novel male germ cell-specific cGMP-dependent protein kinase-anchoring protein by cGMP-dependent protein kinase Ialpha. *J. Biol. Chem.* **275**, 4897–4905 [CrossRef Medline](#)
- Busch, J. L., Bessay, E. P., Francis, S. H., and Corbin, J. D. (2002) A conserved serine juxtaposed to the pseudosubstrate site of type I cGMP-dependent protein kinase contributes strongly to autoinhibition and lower cGMP affinity. *J. Biol. Chem.* **277**, 34048–34054 [CrossRef Medline](#)
- Smith, J. A., Francis, S. H., Walsh, K. A., Kumar, S., and Corbin, J. D. (1996) Autophosphorylation of type Ibeta cGMP-dependent protein kinase increases basal catalytic activity and enhances allosteric activation by cGMP or cAMP. *J. Biol. Chem.* **271**, 20756–20762 [CrossRef Medline](#)
- Alverdi, V., Mazon, H., Versluis, C., Hemrika, W., Esposito, G., van den Heuvel, R., Scholten, A., and Heck, A. J. (2008) cGMP-binding prepares PKG for substrate binding by disclosing the C-terminal domain. *J. Mol. Biol.* **375**, 1380–1393 [CrossRef Medline](#)
- Guo, D. C., Regalado, E., Casteel, D. E., Santos-Cortez, R. L., Gong, L., Kim, J. J., Dyack, S., Horne, S. G., Chang, G., Jondeau, G., Boileau, C., Coselli, J. S., Li, Z., Leal, S. M., Shendure, J., National Heart, Lung, and Blood Institute Grand Opportunity Exome Sequencing Project. (2013) Recurrent gain-of-function mutation in PRKG1 causes thoracic aortic aneurysms and acute aortic dissections. *Am. J. Hum. Genet.* **93**, 398–404 [CrossRef Medline](#)
- Schwaerzer, G. K., Kalyanaraman, H., Casteel, D. E., Dalton, N. D., Gu, Y., Lee, S., Zhuang, S., Wahwah, N., Schilling, J. M., Patel, H. H., Zhang, Q., Makino, A., Milewicz, D. M., Peterson, K. L., Boss, G. R., et al. (2019) Aortic pathology from protein kinase G activation is prevented by an antioxidant vitamin B12 analog. *Nat. Commun.* **10**, 3533 [CrossRef Medline](#)
- Aitken, A., Hemmings, B. A., and Hofmann, F. (1984) Identification of the residues on cyclic GMP-dependent protein kinase that are autophosphorylated in the presence of cyclic AMP and cyclic GMP. *Biochim. Biophys. Acta* **790**, 219–225 [CrossRef Medline](#)
- Francis, S. H., Smith, J. A., Colbran, J. L., Grimes, K., Walsh, K. A., Kumar, S., and Corbin, J. D. (1996) Arginine 75 in the pseudosubstrate sequence of type Ibeta cGMP-dependent protein kinase is critical for autoinhibition, although autophosphorylated serine 63 is outside this sequence. *J. Biol. Chem.* **271**, 20748–20755 [CrossRef Medline](#)
- Feil, R., Bigl, M., Ruth, P., and Hofmann, F. (1993) Expression of cGMP-dependent protein kinase in Escherichia coli. *Mol. Cell Biochem.* **127–128**, 71–80 [CrossRef Medline](#)
- Halbrugge, M., Friedrich, C., Eigenthaler, M., Schanzenbacher, P., and Walter, U. (1990) Stoichiometric and reversible phosphorylation of a 46-kDa protein in human platelets in response to cGMP- and cAMP-elevating vasodilators. *J. Biol. Chem.* **265**, 3088–3093 [Medline](#)
- Butt, E., Abel, K., Krieger, M., Palm, D., Hoppe, V., Hoppe, J., and Walter, U. (1994) cAMP- and cGMP-dependent protein kinase phosphorylation sites of the focal adhesion vasodilator-stimulated phosphoprotein (VASP) in vitro and in intact human platelets. *J. Biol. Chem.* **269**, 14509–14517 [Medline](#)
- Biasini, M., Bienert, S., Waterhouse, A., Arnold, K., Studer, G., Schmidt, T., Kiefer, F., Gallo Cassarino, T., Bertoni, M., Bordoli, L., and Schwede, T. (2014) SWISS-MODEL: modelling protein tertiary and quaternary structure using evolutionary information. *Nucleic Acids Res.* **42**, W252–W258 [CrossRef Medline](#)
- Pires, D. E., Ascher, D. B., and Blundell, T. L. (2014) DUET: a server for predicting effects of mutations on protein stability using an integrated

- computational approach. *Nucleic Acids Res.* **42**, W314–W319 [CrossRef Medline](#)
23. Pires, D. E., Ascher, D. B., and Blundell, T. L. (2014) mCSM: predicting the effects of mutations in proteins using graph-based signatures. *Bioinformatics* **30**, 335–342 [CrossRef Medline](#)
  24. Worth, C. L., Preissner, R., and Blundell, T. L. (2011) SDM—a server for predicting effects of mutations on protein stability and malfunction. *Nucleic Acids Res.* **39**, W215–W222 [CrossRef](#)
  25. Ruth, P., Landgraf, W., Keilbach, A., May, B., Egleme, C., and Hofmann, F. (1991) The activation of expressed cGMP-dependent protein kinase isozymes I alpha and I beta is determined by the different amino-termini. *Eur. J. Biochem.* **202**, 1339–1344 [CrossRef Medline](#)
  26. Ruth, P., Pfeifer, A., Kamm, S., Klatt, P., Dostmann, W. R., and Hofmann, F. (1997) Identification of the amino acid sequences responsible for high affinity activation of cGMP kinase Ialpha. *J. Biol. Chem.* **272**, 10522–10528 [CrossRef Medline](#)
  27. de Jonge, H. R., and Rosen, O. M. (1977) Self-phosphorylation of cyclic guanosine 3':5'-monophosphate-dependent protein kinase from bovine lung. Effect of cyclic adenosine 3':5'-monophosphate, cyclic guanosine 3':5'-monophosphate and histone. *J. Biol. Chem.* **252**, 2780–2783 [Medline](#)
  28. Vallur, R., Kalbacher, H., and Feil, R. (2014) Catalytic activity of cGMP-dependent protein kinase type I in intact cells is independent of N-terminal autophosphorylation. *PLoS ONE* **9**, e98946 [CrossRef Medline](#)
  29. Francis, S. H., Morris, G. Z., and Corbin, J. D. (2008) Molecular mechanisms that could contribute to prolonged effectiveness of PDE5 inhibitors to improve erectile function. *Int. J. Impot. Res.* **20**, 333–342 [CrossRef Medline](#)
  30. Wolfertstetter, S., Huettner, J. P., and Schlossmann, J. (2013) cGMP-dependent protein kinase inhibitors in health and disease. *Pharmaceuticals* **6**, 269–286 [CrossRef Medline](#)
  31. Valtcheva, N., Nestorov, P., Beck, A., Russwurm, M., Hillenbrand, M., Weinmeister, P., and Feil, R. (2009) The commonly used cGMP-dependent protein kinase type I (cGKI) inhibitor Rp-8-Br-PET-cGMPS can activate cGKI in vitro and in intact cells. *J. Biol. Chem.* **284**, 556–562 [CrossRef Medline](#)
  32. Taylor, M. S., Okwuchukwasanya, C., Nickl, C. K., Tegge, W., Brayden, J. E., and Dostmann, W. R. (2004) Inhibition of cGMP-dependent protein kinase by the cell-permeable peptide DT-2 reveals a novel mechanism of vasoregulation. *Mol. Pharmacol.* **65**, 1111–1119 [CrossRef Medline](#)
  33. Osborne, B. W., Wu, J., McFarland, C. J., Nickl, C. K., Sankaran, B., Casteel, D. E., Woods, V. L., Jr., Kornev, A. P., Taylor, S. S., and Dostmann, W. R. (2011) Crystal structure of cGMP-dependent protein kinase reveals novel site of interchain communication. *Structure* **19**, 1317–1327 [CrossRef Medline](#)
  34. Kim, J. J., Lorenz, R., Arold, S. T., Reger, A. S., Sankaran, B., Casteel, D. E., Herberg, F. W., and Kim, C. (2016) Crystal structure of PKG I:cGMP complex reveals a cGMP-mediated dimeric interface that facilitates cGMP-induced activation. *Structure* **24**, 710–720 [CrossRef Medline](#)
  35. Herberg, F. W., Dostmann, W. R., Zorn, M., Davis, S. J., and Taylor, S. S. (1994) Crosstalk between domains in the regulatory subunit of cAMP-dependent protein kinase: influence of amino terminus on cAMP binding and holoenzyme formation. *Biochemistry* **33**, 7485–7494 [CrossRef Medline](#)
  36. Badireddy, S., Yunfeng, G., Ritchie, M., Akamine, P., Wu, J., Kim, C. W., Taylor, S. S., Qingsong, L., Swaminathan, K., and Anand, G. S. (2011) Cyclic AMP analog blocks kinase activation by stabilizing inactive conformation: conformational selection highlights a new concept in allosteric inhibitor design. *Mol. Cell. Proteomics* **10**, M110.004390 [CrossRef](#)
  37. Simanshu, D. K., Nissley, D. V., and McCormick, F. (2017) RAS proteins and their regulators in human disease. *Cell* **170**, 17–33 [CrossRef Medline](#)
  38. Han, X. (2014) Constitutively active chemokine CXCR2 receptors. *Adv. Pharmacol.* **70**, 265–301 [CrossRef Medline](#)
  39. Malik, R. U., Ritt, M., DeVree, B. T., Neubig, R. R., Sunahara, R. K., and Sivaramakrishnan, S. (2013) Detection of G protein-selective G protein-coupled receptor (GPCR) conformations in live cells. *J. Biol. Chem.* **288**, 17167–17178 [CrossRef Medline](#)
  40. Schwappacher, R., Rangaswami, H., Su-Yuo, J., Hassad, A., Spittler, R., and Casteel, D. E. (2013) cGMP-dependent protein kinase Ibeta regulates breast cancer cell migration and invasion via interaction with the actin/myosin-associated protein caldesmon. *J. Cell Sci.* **126**, 1626–1636 [Cross-Ref Medline](#)
  41. Zhuang, S., Nguyen, G. T., Chen, Y., Gudi, T., Eigenthaler, M., Jarchau, T., Walter, U., Boss, G. R., and Pilz, R. B. (2004) Vasodilator-stimulated phosphoprotein activation of serum-response element-dependent transcription occurs downstream of RhoA and is inhibited by cGMP-dependent protein kinase phosphorylation. *J. Biol. Chem.* **279**, 10397–10407 [CrossRef Medline](#)
  42. Higuchi, R., Krummel, B., and Saiki, R. K. (1988) A general method of in vitro preparation and specific mutagenesis of DNA fragments: study of protein and DNA interactions. *Nucleic Acids Res.* **16**, 7351–7367 [CrossRef Medline](#)
  43. Kim, C., Cheng, C. Y., Saldanha, S. A., and Taylor, S. S. (2007) PKA-I holoenzyme structure reveals a mechanism for cAMP-dependent activation. *Cell* **130**, 1032–1043 [CrossRef Medline](#)
  44. Marsh, J. J., Guan, H. S., Li, S., Chiles, P. G., Tran, D., and Morris, T. A. (2013) Structural insights into fibrinogen dynamics using amide hydrogen/deuterium exchange mass spectrometry. *Biochemistry* **52**, 5491–5502 [CrossRef Medline](#)